SERAMİK
Journal of the Turkish Ceramics Society

Seramik - Journal of the Turkish Ceramics Society, 2 (1) 7-18 (2022)

Özgün Araştırma Makalesi / Original Research Article

Utilization of Carbon Fibers in Glass-Ceramic Coatings

Büşra Karakaş[1], Nurullah Çöpoğlu[1,2], Hatice Gökdemir[2], Tamer Cengiz[1,2] and Buğra Çiçek[1]

[1] *Yıldız Technical University, Department of Metallurgy and Materials Science Engineering, 34210 Esenler, Istanbul, Turkey*

[2] *Akcoat R&D Center, Enamel Coatings Division, 2nd IZ,54300, Sakarya, Turkey*

Sorumlu Yazar / Corresponding Author
Buğra Çiçek
bcicek@yildiz.edu.tr

Makale Bilgisi / Article Info
Sunulma / Received : 15.08.2021
Düzeltme / Revised : 21.03.2022
Kabul / Accepted : 24.03.2022

Anahtar Kelimeler
Cam-seramik
Kaplama
Karbon fiber
Mekanik direnç

Keywords
Glass-ceramic
Coating
Carbon fiber
Mechanical resistance

ORCID
Büşra Karakaş
https://orcid.org/0000-0003-4646-3222
Nurullah Çöpoğlu
https://orcid.org/0000-0001-9328 7511
Hatice Gökdemir
https://orcid.org/0000-0001-8195-4153
Tamer Cengiz
https://orcid.org/0000-0002-3642-1064
Buğra Çiçek
https://orcid.org/0000-0001-8195-4153

Abstract

Glass-ceramic coatings are inorganic systems obtained by controlled crystallization by heat treatment of parent glasses coated on steel substrates. This type of coating possesses superior engineering properties among other coating systems, such as strong adhesion between enamel and steel substrate (adherence index>95%), resistance to high temperature (up to 1000°C), chemical corrosion (3-4 mg.dm^{-2} 6% citric acid), while maintaining aesthetical properties. The brittle fracture behavior of glass-ceramic coatings reduces their impact and abrasion resistance, which has a detrimental influence on the stability and longevity of the entire system. Carbon fibers possess excellent properties such as low weight (1.76 g/cm^3), high specific strength (2900-3000 MPa) and modulus (200-220 GPa), and low linear expansion coefficient (-1.20x10^{-6}/°C) except for weak resistance of oxidation behavior as a reinforcement in composite materials. In this study, three different alkaline borosilicate systems were investigated. In each formulation, two different samples containing 0.06%, and 1% wt. carbon fiber was incorporated into the matrix as a mill additive. The samples were coated on the steel substrates by the wet coating technique and fired at 860°C for 6 min. The coatings were characterized for morphological, phase, thermal properties by means of SEM-EDS, XRD, and heating microscope, respectively. In this study, when the carbon fiber ratio is 1% wt., the hardness of GC1, GC2 and GC3 samples increases to 763.8, 889 and 865.2 VH, respectively. On the other hand, morphological features of the coatings are negatively affected.

Cam-Seramik Kaplamalarda Karbon Elyaf Kullanımı

Özet

Cam-seramik kaplamalar, çelik yüzeyler üzerine kaplanmış ana camların ısıl işlem uygulanarak kontrollü kristalizasyonuyla elde edilen inorganik sistemlerdir. Bu tür kaplamalar, diğer kaplama çeşitleri arasında üstün mühendislik özelliklerine sahiptir; çelik tabaka ile güçlü yapışma özelliği gösterirler (aderans indeksi>%95), yüksek sıcaklığa (1000°C'ye kadar) ve kimyasal korozyona karşı (3-4 mg.dm^{-2} 6% sitrik asit) fiziksel özelliklerini de koruyarak direnç gösterirler. Cam-seramik kaplamaların gevrek kırılma davranışı, darbeye ve aşınmaya gösterdikleri direnci azaltır ve bu durum ürün güvenirliliği ve kullanım ömrü üzerinde olumsuz bir etkiye sahiptir. Karbon fiberler kompozit malzemelerde takviye olarak kullanıldığında, zayıf oksidasyon dirençleri hariç üstün özellikler sergilerler. Bu özellikler düşük ağırlık (1.76 g/cm^3), yüksek özgül mukavemet (2900-3000 MPa), modül (200-220 GPa) ve düşük doğrusal genleşme katsayısı (-1.20x10^{-6}/°C) olarak sıralanabilir. Bu çalışmada üç farklı alkali borosilikat sistemi incelenmiştir. Her bir sisteme, ağırlıkça %0.06 ve %1.00 karbon fiber, değirmen katkısı olarak ilave edilmiştir. Numuneler yaş kaplama tekniği ile çelik plakalara kaplanmıştır ve 860°C sıcaklığında 6 dakika boyunca ısıl işlem uygulanmıştır. Kaplamaların morfolojik, faz, termal özellikleri sırasıyla SEM-EDS, XRD ve ısı mikroskobu aracılığıyla belirlenmiştir. Bu çalışmada, karbon fiber oranı ağırlıkça %1.00 olduğunda, GC1, GC2 ve GC3 numunelerinin sertlik değerleri sırasıyla 763.8, 889 and 865.2 VH değerlerine yükselir. Ancak, kaplamaların morfolojik özellikleri kötü etkilenmiştir.

1. INTRODUCTION

Glass-ceramics (GCs) are obtained by controlled heat treatment process of parent glass system with appropriate composition generally between the glass-transition temperature (T_g) and the melting point (T_m) and form various types of crystals in its structure[1]. The glass matrix undergoes controlled crystallization to the lower energy, resulting in developing randomly oriented submicrometric final grain sizes generally without voids, microcracks, or porosity with nucleating agents[2]. Glass-ceramics (GCs) with functional properties can be produced in consequence of a composition of the characteristics of glasses with the advantages of crystalline phases. Some of those are high-temperature and abrasion resistance, high strength, machinability, biocompatibility[3, 4].

Glass-ceramic coatings (GCCs) can be applied on ferrous substrates by wet/dry methods. After the GCCs are applied to the substrate, heat treatment is applied; drying and crystallization[5]. Chemical plants, hydrogen power, water heaters employ this type of coating where great durability and chemical corrosion protection are required[6,7]. Glass-ceramic coatings (GCCs) offer the ferrous components a wide range of color options, and the resultant product's aesthetic features are kept even in hard environments[8].

Abrasion is the most common deformation mechanism in the coated surfaces caused by brittle fracture attitude glass-ceramic coatings (GCCs) of glassy nature[9,10]. As a result of degrading the coated surface's glassy layer, porosity forms at the interface, lowering the interface's stability, chemical resistance, and aesthetic attributes under extreme conditions. Several studies have been published in the literature to enhance the abrasion resistance and mechanical properties of inorganic coating systems. These studies include changes to the system's composition[9], as well as the addition of mill additives[11] and particles.[12–14] According to the studies, the engineering properties of the coatings depend on some variables such as firing conditions, the mismatch stress between the additive and parent system, quantity, and the size of additives.

Carbon fiber reinforced glass matrix composites indicate a wide variety of features including for structural application high strength, high stiffness, excellent toughness, low density, and unique tribological behavior.[15–26] However, the main disadvantage of this type of composite is the limited oxidation resistance capability in an oxidizing atmosphere at high temperatures. During the crack propagation, debonding of fibers and pull-out is actualized when a crack reaches the carbon fibers, hence strain energy release rate is increasing for toughness mechanism.[27,28] In this situation, composite failure strain is equal to that of the fibers with significant fiber pull out, which means improved composite toughness. Composite ultimate failure strain is greater than that of the matrix alone[29]. In addition, for optimum performance in carbon fiber reinforced glass composites, fiber/matrix interfacial adhesion should be kept in intermediate value.[30]

In this study, the effects of reinforcement of carbon fiber on the morphological, thermal, and mechanical properties of glass-ceramic coatings (GCCs) were investigated.

The study's objective is to improve the hardness of the glass-ceramic coatings (GCCs). In this approach, the increased hardness and toughness of glass-ceramic coatings (GCCs) assist to enhance the system's durability.

2. MATERIALS & METHODS

2.1. Materials

The substrates used in the study for the glass-ceramic coating were steel sheets that are EN 10209 Grade DC06EK cold rolled types with the dimensions of 10 cm x 10 cm x 0.15 cm. The steel substrates were subjected to surface cleaning before the coating process by degreasing.

The alkali borosilicate frit systems (available for controlled crystallization for GCC) were provided by Akcoat Advanced Chemical Coating Materials (Sakarya, Turkey). The frits were crushed, and the ball-milled down to a 60-mesh sieve (250 µm) by adding mill additives (clay, boric acid, and sodium nitrite). The recipes used in the study are given in Table 1. The features of the carbon fiber are shown in Table 2, and the carbon fiber was provided by DowAksa Advanced Composites (Yalova, Turkey).

Table 1 Chemical compositions of the studied samples.

Constituents in the compositions	GC1 (%wt.)	GC2 (%wt.)	GC3 (%wt.)
R_2O (R: Na, K, Li)	21.25	13.00	16.00
RO (R: Ca, Mg, Ni, Co, Cu, Mn)	4.25	5.00	8.50
R_2O_3 (R: Fe, Al, B)	13.25	9.25	11.25
RO_2 (R: Si, Ti, Zr)	58.50	71.25	63.25
R (R: F)	2.75	1.50	1.00

2.2. Experimental Design

In this study, three different alkali borosilicate system was used. These were coded as GC1, GC2, GC3. For each system, carbon-fiber free, containing %0.06 and %1.00 wt. carbon fiber content samples were prepared. The milled carbon fiber was incorporated into the compositions as a mill additive. The samples codes of the GCC-CFs used in the study are shown in Table 3.

The GC slip was prepared by mixing the frit powder with 40% (70-80 mL) of water of total powder volume. After this process, the slip was applied on the surfaces of the pretreated steel substrates by the dipping for GC1 and GC2 and spraying technique for GC3. These techniques were chosen according to the characteristics of the compositions. The coated samples were dried in an oven for 5 min. at 110°C to evaporate the water and, then fired at 860°C for 6 min. for crystallization.

Table 2 Properties of carbon fiber used in the study.

Diameter (µm)	Length (µm)	Density (g/cm^3)	Tensile Strength (MPa)
1 –10	1 –50	1.76	2900 –3000

Table 3 Sample codes and carbon fiber content in the samples.

Sample Code	Addition of CF (wt.)
GC1	Reference sample No. 1
GC1-6	%0.06 Carbon Fiber
GC1-10	%1.00 Carbon Fiber
GC2	Reference sample No. 2
GC2-6	%0.06 Carbon Fiber
GC2-10	%1.00 Carbon Fiber
GC3	Reference sample No. 3
GC3-6CF	%0.06 Carbon Fiber
GC3-10CF	%1.00 Carbon Fiber

2.3 Characterization Studies

XRD analysis with CuKα radiation, scanning range (2θ) of 15°–70° (Rigaku Miniflex 600) performed on pelleted powders. The microstructure of GCCs was observed by Jeol JSM-6060LV scanning electron microscopy/SEM equipped with EDS. For scanning electron microscopy (SEM) analysis, an acceleration voltage of 15 kV was used at working distances of 9.5- and 10-mm. Color values and the color of the samples were evaluated with Konica Minolta CM-700d Spectrophotometer in terms of L*, a*, b*, and ΔE. Color measurements were determined for four different points. The color values are the mean of four measurements. The total difference or distance in the CIELAB diagram can be expressed as a single value known as ΔE*.[31]

$$\Delta E^* = [(\Delta L^2) + (\Delta a^2) + (\Delta b^2)]^{1/2} \quad (1)$$

Gloss was evaluated with a TQC Sheen Polygloss gloss meter device at 60° in four different points. The results are the mean of four measurements. The coated specimens were tested by the falling steel ball impact test by BS EN 10209 standard for determination adherence feature of the com. A hemispherical punch with a diameter of 1.5 kg and a diameter of 22 mm was dropped on the sample surface at a height of 300 mm. The degree of adherence was interpreted with impact signs according to ratings ranging from 5 (poor adherence) to 1 (excellent adherence).

Heating microscope observes the sintering behaviors of the glass-ceramic coatings, a heating microscope (ODHT-HSM 1600/50, Misura 3.32) was used. The sintering and melting temperatures of the coatings were determined by heating the powdered samples to 900 °C at a rate of 10 °C/min.

Microhardness was measured with the Vickers hardness test method (Struers Duramin A300). In the Vickers method, the pyramid stinging tip with 136° of apex angle between the counter-surfaces of the pyramid having a square base is stung onto the sample for 10 seconds under force (F). 100 grams of the load was applied to the samples during the procedures. After removing the load, two diagonal lengths of the trace (d1 and d2) on the material are measured using a microscope, and the arithmetic mean (d) is calculated. This procedure has repeated a minimum of 10 times for each load and the mean value is calculated. Because only the hardness of the GCs was examined in this study, hardness was measured in the cross-section of the coating to avoid any contribution from the substrate hardness. In the Vickers test method, hardness was measured at 5 different points, and 5 results were averaged.

3. RESULTS AND DISCUSSION

3.1. Phase Analysis

Fig. 1 presents the XRD patterns of the GC1, GC2, and GC3 composition with different carbon fiber content heat-treated at their crystallization regime. For GC1, GC2, and GC3 formulations, SiO_2 and SiC, SiO_2 and $ZrSiO_4$, SiO_2 phase are obtained, respectively. The addition of carbon fiber to the compositions was not effective in crystallization formation. Since carbon fiber was used at very low percentages, the carbon fiber may not have been observed due to the crystallinity of other phases. SiC crystal phase was obtained due to steel substrate use during the crystallization process. The steel substrate becomes 70% austenitic, hence dissolved carbon in the austenite phase can diffuse more rapidly from the steel to the glass/metal interface[32]. This diffusion may lead to SiC crystal phase formation in GC1. In the GC3 composition, only SiO_2 crystal formation was obtained because GC3 was formed in the high silica content area in the ternary diagram of the sodium borosilicate system.

3.2. Microstructural Analysis

Porosity and bubble structure in the glass-ceramic coating has an important influence on the quality of the glass-ceramic coating. Porosity and bubbles are mainly created due to the outgassing during the heat treatment[29]. At the beginning of the heat-treatment process, the coating surface is fused, and gaseous products are trapped in the glass-ceramic coating. With the continued firing causes to the expanse of the gas, then bubble structures are formed. At the final stage of heat treatment, some bubbles rise to the surface of the coating and cause flaws in the surface because of the low viscosity of the glass-ceramic coating[33]. In addition, water vapor is formed after the decomposition of clay. Before the firing treatment, the melting frit is cooled, the vitreous layer is formed, and water vapor is trapped as a fine bubble.

The pore dispersion and size are related to the firing temperature, the viscosity of the slip, and additives[9]. Due to the high viscosity of the melting coating, the bubbles cannot grow at the firing temperature, hence the bubble size becomes small. In the GC, few bubbles form under insufficient heat-treatment settings, while very large bubbles or no bubbles form under overfired circumstances[29]. Underfired GCs have poor adhesion to the substrate, making the coating susceptible to cracking. On the other hand, brittle behavior is caused by the formation of large bubbles in the GCs. As a result, the best condition for GCs is a properly fired coating with optimal size and homogeneous bubble structure[33].

In Fig. 2 SEM images belonging to GC1, GC2, and, GC3 samples are shown, and the bubble formation due to outgassing is recognizable. The thickness of the samples is 250±50 µm. EDS images of Si, O, Na, Al, Zr in the carbon-free samples are shown in Fig. 2. Si, O, Na, Al, Zr are the main elements of the GCCs. The color differences in the cross-section of GCCs can be seen due to undissolved silicate crystals from mill additives or formed crystals in the controlled crystallization process. In Fig. 3 SEM images belonging to GC1-6CF, GC2-6CF, and GC3-6CF are shown, and the bubbles can be seen in cross-section images due to outgassing.

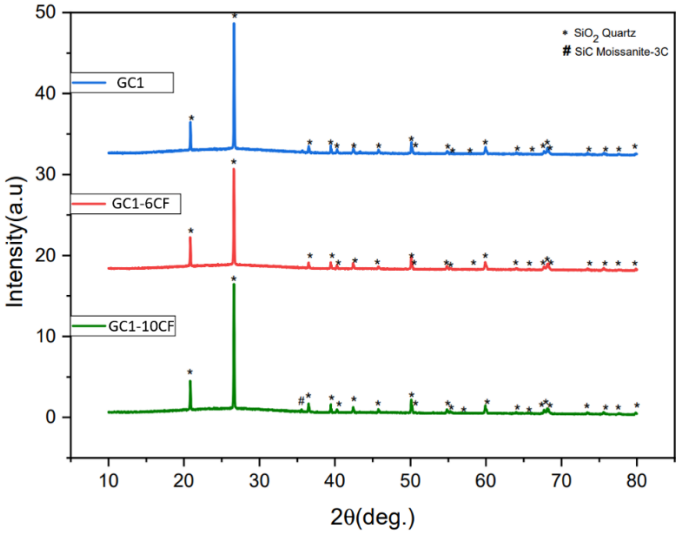

(A)

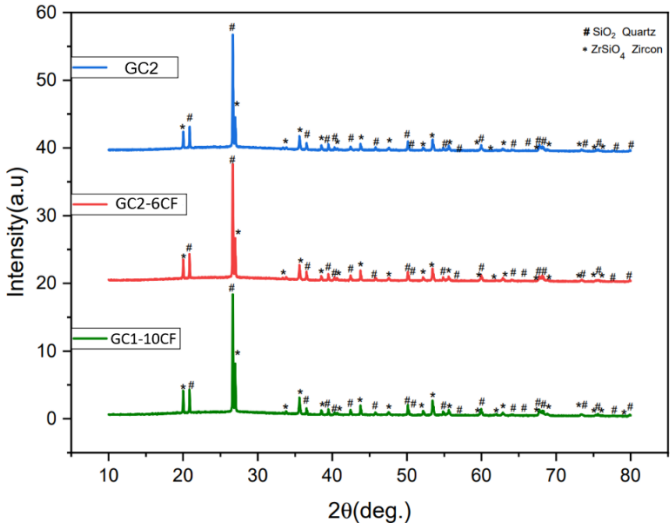

(B)

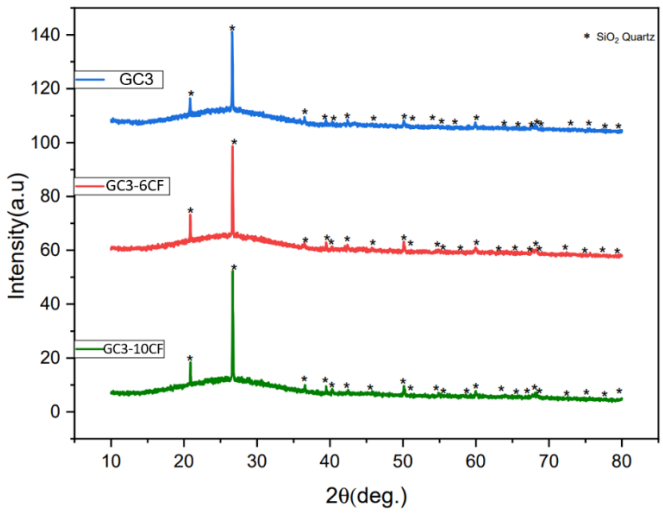

(C)

Figure 1. XRD patterns of the studied samples with different carbon fiber ratios. A) GC1 samples B) GC2 samples C) GC3 samples.

The thicknesses of the coating contained 0.06% wt. carbon fiber is in the range of 250–350 µm. The inclusion of carbon fiber has no discernible effect on the size and distribution of bubble structure.

However, when carbon fiber is used in GCs, these bubbles are filled with carbon fiber as an agglomeration, or carbon fiber creates its cavity because of oxidation. Therefore, due to agglomeration, the size of carbon fiber increases from an average of 10 µm to 50 µm, as shown in Fig. 3. The use of carbon in glass-ceramic coatings increases the hardness of components in both circumstances. Glass-ceramic coatings are reasonably hard, but their mechanical resistance is restricted due to the brittle nature of the glass matrix, which allows for the formation and propagation of cracks.

The toughness of ceramics is characterized by the indentation fracture toughness (K_{IC}), which is an indication of the ease cracks propagate in the material[32]. Vickers hardness test can be used to determine a parameter relating to the material's fracture toughness and hardness[33,34]. The fracture toughness mechanism of ceramic materials can be determined by the relationship between the applied force on the Vickers hardness test and the average crack length on the fracture process[35]. In this study, filling the formed bubbles with carbon fiber leads to an increment in hardness values because this stress was diffuse in this formation of carbon fiber in the bubbles when the Vickers hardness test was applied as an external force. It is shown in Figure 4 and applies to all formulations with various carbon fiber percentages. When the carbon fiber ratio is 1% wt., the hardness of GC1 samples increases from 737.40 to 763.80 VH. In GC2 samples, the hardness is increased from 816.60 to 889.0 VH when the carbon fiber ratio is 1% wt. In GC3 samples, the hardness is increased from 831.60 to 865.20 VH when the carbon fiber ratio is 1% wt. The standard deviation values are given in Fig. 4. The values are 71.7, 14.08, and 27.03 for GC1, GC1-6, GC1-10, respectively. For GC2, GC2-6, and GC2-10, the standard deviation values are 34.50,73.60, and 34.80. The values are 11.70, 13.74, and 69.80 for GC3 GC3-6, GC3-10, respectively.

SEM images of the studied samples' surfaces are shown in Fig. 5. Three different commercial glass-ceramic compositions are employed as a reference sample in this investigation, and the compositions indicate their characteristic features. Undissolved SiO_2 crystals are marked in Fig. 5a, g belongs to GC1 and GC3 glass-ceramic compositions, also be confirmed by XRD results. SEM images cross-sections of $ZrSiO_4$ crystals embedded in the glass matrices in GC2 samples are shown in Fig. 2b. With the increasing carbon fiber content in compositions, the flaws and disorders are increasing on the surfaces regardless of the type of glass-ceramic coating. Carbon fiber is resistant to oxidation until 500°C, after this temperature heat-treatment was continued and the reaction of oxygen causes CO_2 outgassing, resulting in flaws on the surfaces.

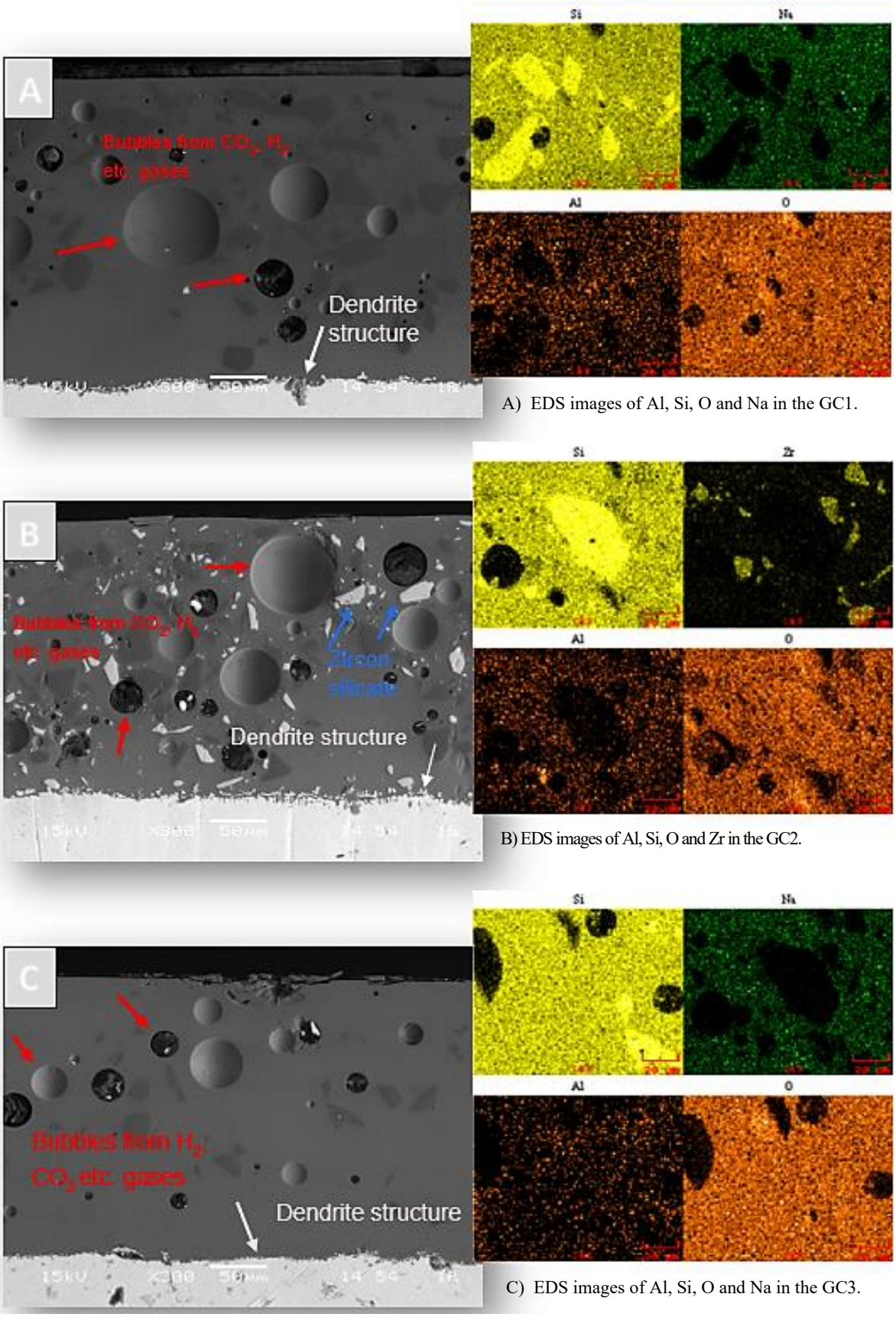

A) EDS images of Al, Si, O and Na in the GC1.

B) EDS images of Al, Si, O and Zr in the GC2.

C) EDS images of Al, Si, O and Na in the GC3.

Figure 2. SEM/EDS cross-sections images of the studied samples. A) GC1 B) GC2 C) GC3.

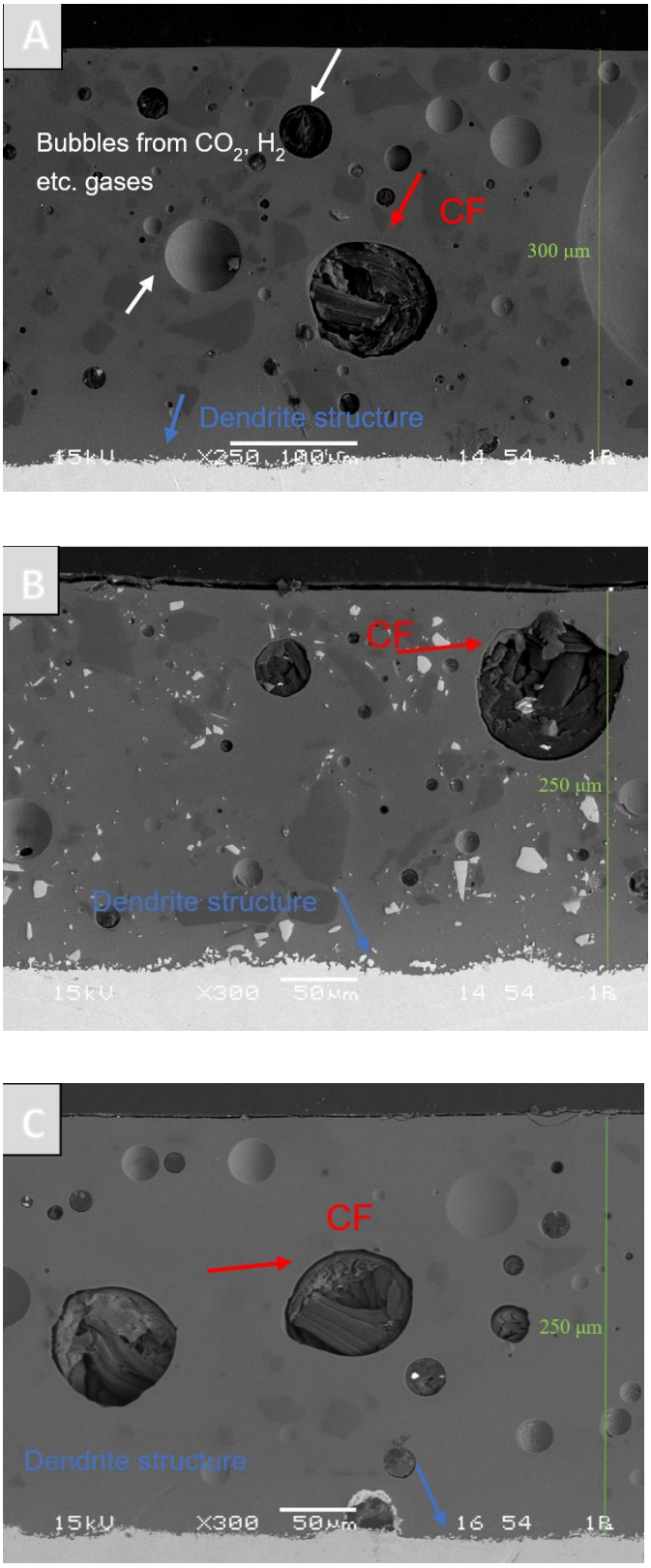

Figure 3. SEM cross-sections images of the studied samples. A) GC1-6CF B) GC2-6CF C) GC3-6CF..

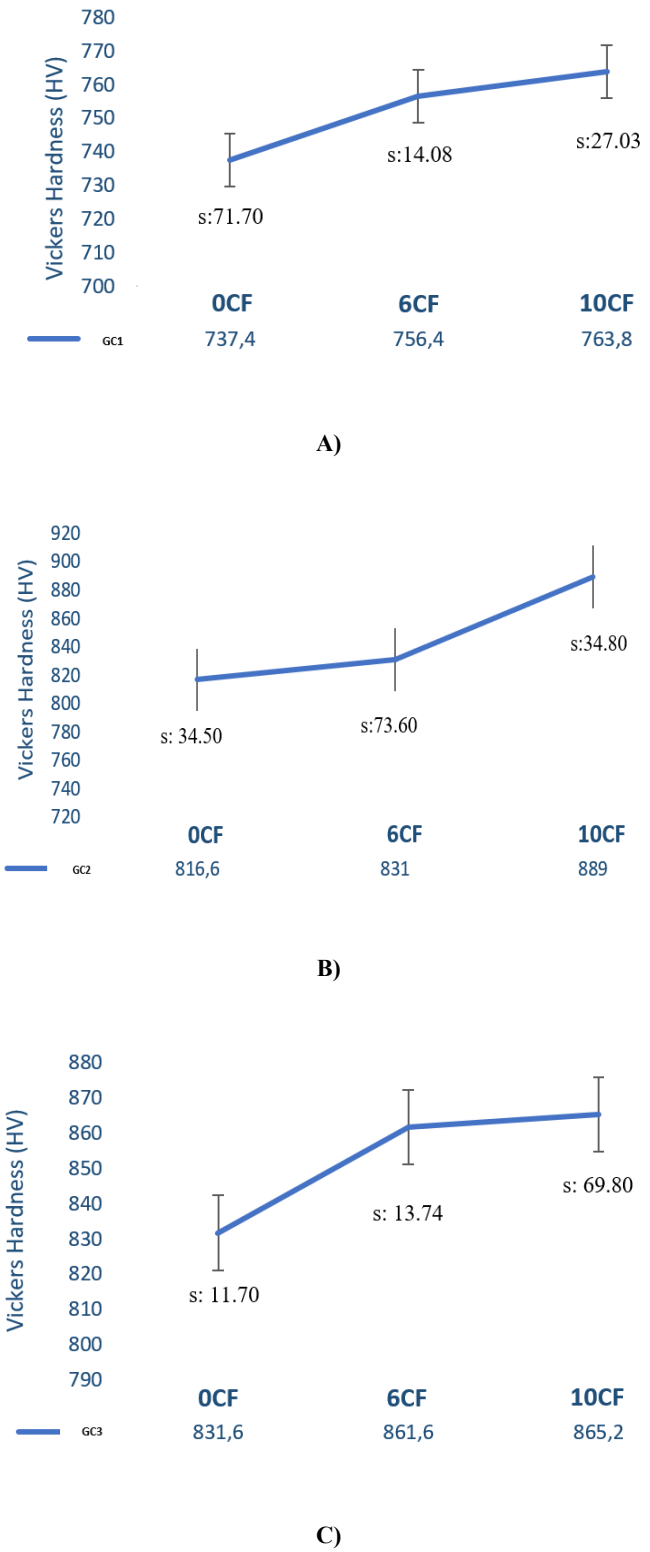

Figure 4. Vickers hardness test result of studied samples. A) GC1 samples with 6CF and 10CF C) GC2 samples with 6CF and 10CF C) GC3 samples with 6CF and 10CF.

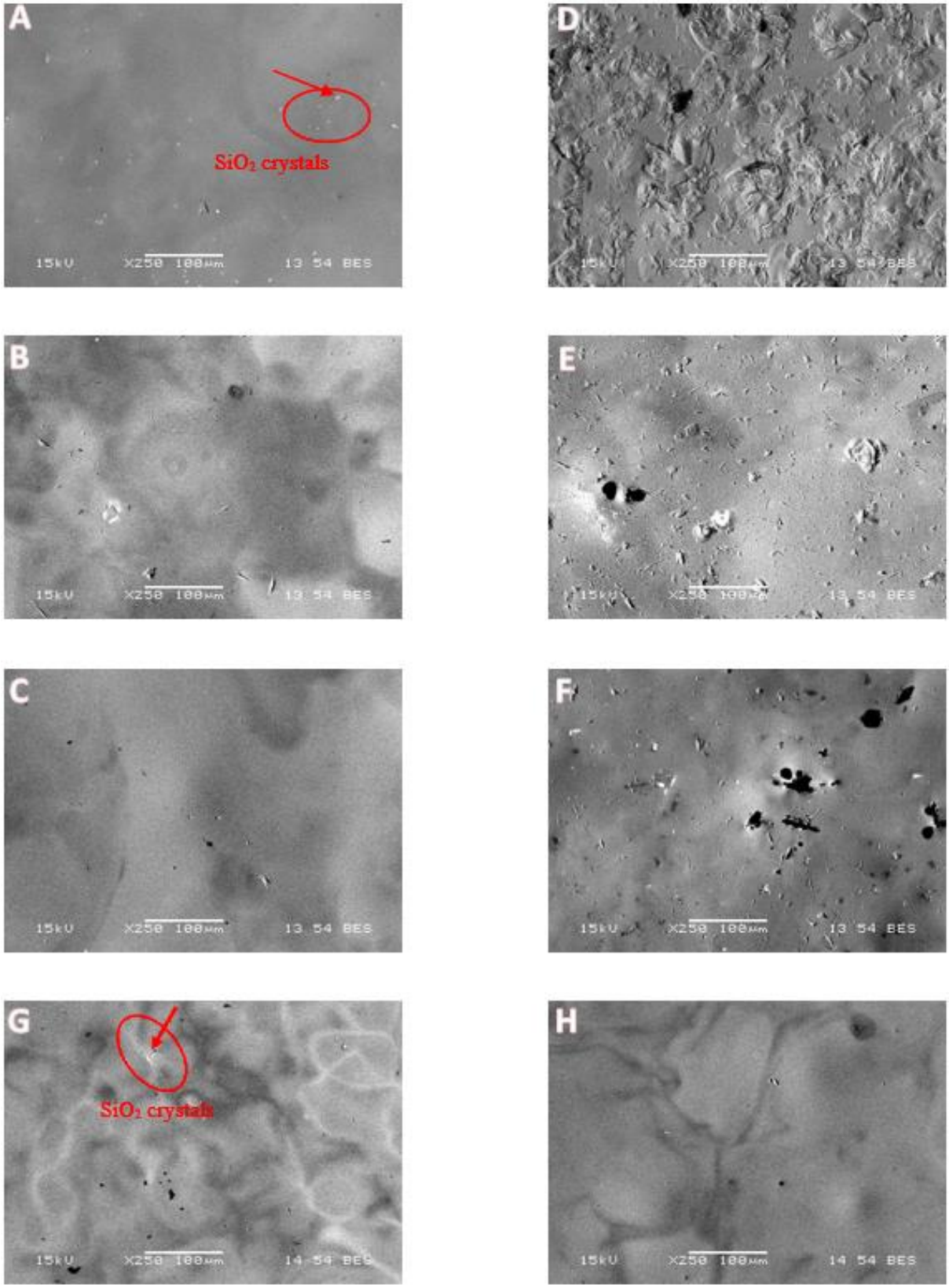

Figure 5. SEM images of the studied samples surfaces. A) GC1 B) GC1-6CF C) GC1-10CF D) GC2 E) GC2-6CF F) GC2-10CF G) GC3 H) GC3-6CF.

3.3. Gloss and color parameters

This increment of flaws and disorders on the surface affects the gloss and color parameters, as shown in Fig.7. In the study, the color differences between the reference samples and samples containing carbon fiber are determined by equation 1 and ΔL, Δa, Δb values from Table 4. In CIE color notation, ΔL* values indicate the difference in lightness and darkness; a positive deviation from ΔL* means a lighter color. Δa* values indicate difference on a red or green axis; a positive deviation from Δa* means a redder color while a negative deviation from Δa* means a greener color. Δb* values represent difference on the yellow or blue axis whereas a positive deviation from Δb* means a yellower color, and negative deviation from Δb* means a bluer color[31].

For each formulation, Fig. 7a shows a color comparison of carbon fiber-containing samples and reference samples. According to these results, the addition of carbon to the compositions affects the color values for each carbon fiber content in the samples. For GC1 and GC3 formulations with different carbon fiber content shows similar color changes in comparison of reference samples and %1.00 and %0.06wt.CF. On the other hand, the ΔE values of GC2-6CF and GC2-10CF differ significantly as the GC2-10CF samples are much brighter (Table 4).

Table 4 Color values of studied samples.

Compared Samples	ΔL*	Δa*	Δb*
GC1 &6CF	-0.575	0.28	-0.5825
GC1 &10CF	-0.565	-0.6	1.5975
GC2 &6CF	-0.025	-0.5	-0.7175
GC2 &10CF	7.76	-0.7	1.1225
GC3 &6CF	6.82	-0.1	-1.2325
GC3 &10CF	8.2525	-1.3	3.4925

Gloss values of the studied samples are shown in Table 5 and the variation of gloss values with carbon fiber addition is shown in Fig. 7b. The carbon fiber impairs the gloss values of the samples as associated with the visual appearances of the surface of the coatings in Fig. 5. Being the gloss, a characteristic depends on the surface's light reflection, as well as on the surface roughness. Although the roughness feature is not evaluated in this study, the presence of carbon fiber caused a decrease in gloss values due to the flaws created by the outgassing caused by oxidation of the fiber.

Table 5 Gloss values of studied samples.

	GLOSS (60°)
GC1	39.15
GC1-6CF	33.00
GC1-10CF	28.175
GC2	32.93
GC2-6CF	31.10
GC2-10CF	12.90
GC3-CF	70.55
GC3-6CF	44.92
GC3-10CF	41.65

3.4. Thermal Behavior

Fig. 8 shows a result of the heating microscope belonging to GCs with different carbon fiber content. The addition of carbon fiber has an insignificant effect on the thermal behavior of the samples. However, carbon fiber changes the characteristic temperature values obtained by the heating microscope analysis of glass-ceramic coatings. For example, the melting temperatures of GC1-10 (850°C) and GC2-10 (860°C) are greater than the samples containing other CF ratios, according to heating microscope results, while GC3-10 (812°C) is equal to GC3. The softening temperatures of GC1-10 (730°C), GC2-10 (748°C), and GC3-10 (704°C) are higher than their composition groups. Sphere temperatures of GC1-6 (788°C) are higher than GC1-10 (768°C) and GC1 (786°C) (Fig.8A). For sphere temperatures of GC2-6 (796°C) is higher than GC2-10 (782°C) and GC2 (764°C) (Fig.8B). In GC3 composition, adding to the carbon fiber (1%wt.) enhances thermal behavior, as shown in Fig.8C. The temperatures defined by the microscope are the temperature at which the sample reaches a dimensional change from the first image acquired. Therefore, in the heating microscopy results, the increase in the dimensional changes of the components containing 1% CF is greater because they have more oxidic components.

Figure 6 SEM images of the GC3-10CF sample surface are shown. The presence of carbon fiber can be seen on the surface of the GC3-10 with an EDS image. In the glass crystallization mechanism, increasing T causes a decrease in viscosity[37]. Therefore, carbon fiber can penetrate the glass matrix and rise to the surface in GC3 samples as the samples are heat-treated after their melting temperatures. The melting point of the GC3-10CF is 812°C according to heating microscope results (Fig.8). In this study, the crystallization temperature was chosen at 860°C for the samples. After the melting point of the samples, heat treatment was continued, and early crystallization was achieved in GC3 samples. This early crystallization effect can be observed on the surfaces of the samples in Figures 5g, h, and Fig. 6. GC3 samples show low thermal resistance according to heating microscope results in Fig.8.

Glass-ceramics are bonded to a metal substrate by thermal fusion at temperatures above 800°C. At these temperature ranges, chemical redox reactions occur between the oxide layer of the steel and the metal oxides in the glass-ceramic compositions and thus bonding is achieved. Considering these reactions and the thermal behavior of standard samples, the crystallization temperature of 860°C was chosen for each type of GC used in the study.

3.5 Adherence

During heat-treatment several chemical processes are actualized such as diffusion of alkali ions F^-, Co^{2+}, and Fe^{2+}, formation of Fe^- oxidation on the steel surface, formation of Fe_xCo_y dendrites (anchor points), a saturation of FeO/Fe_3O_4 at the GC, and steel interface, O^{2-} penetration, etc. These dendrites, showing the chemical adhesion between the coating and the metal substrates, are indicated in cross-sections in the SEM images of the samples in Fig. 2 and 3. These chemical reactions provide a strong adherence between the substrate and the coating. This chemical bond is one of the most important parameters of the coating system. In Fig. 9, results of the GCCs with different carbon fiber ratios

after the impact test process is shown. This test presents adherence between the substrate and the coating. This chemical bond is one of the most important parameters of the coating system. In Fig. 9, results of the GCCs with different carbon fiber ratios after the impact test process is shown. This test presents adherence between the substrate and the coating.

According to these results, the quantities of carbon fibers do not significantly change the results of the impact test. In the impact test, the result is evaluated according to the 5 different categories: 5) poor adherence, 4) fair adherence, 3) good adherence, 2) very good adherence, and 1) excellent adherence (BS EN 10209). These categories are determined by the amount of glass-ceramic coating particles remaining on the metal substrate after the impact test process. For example, the appearance of only the shiny metal substrate indicates that no adhesion was obtained. Figures 9a, d, and h are the reference samples for each formulation, these samples show very good adhesion, which means that the glass-ceramic coating particles adhere to at least 70% to 80% of the area of impact. Carbon fiber has no significant effect on adherence for 1 wt. %CF and 0.06CF ratios, according to these results, because adherence features are similar for each formulation with varying carbon fiber ratios. In the study, all samples can be categorized to class 2 adherence according to BS EN 10209 standard, and further evidenced by dendrite formations, as shown in Fig. 3 and 2.

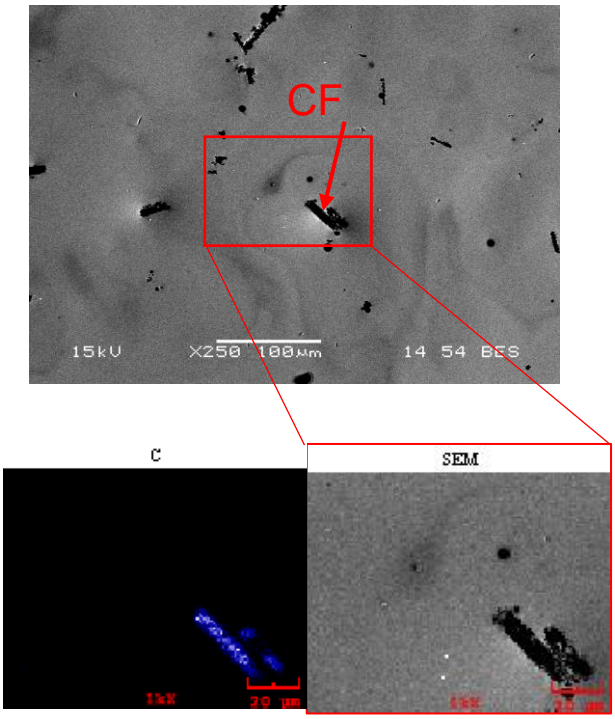

Figure 6. SEM images of the studied GC3-10CF surface.

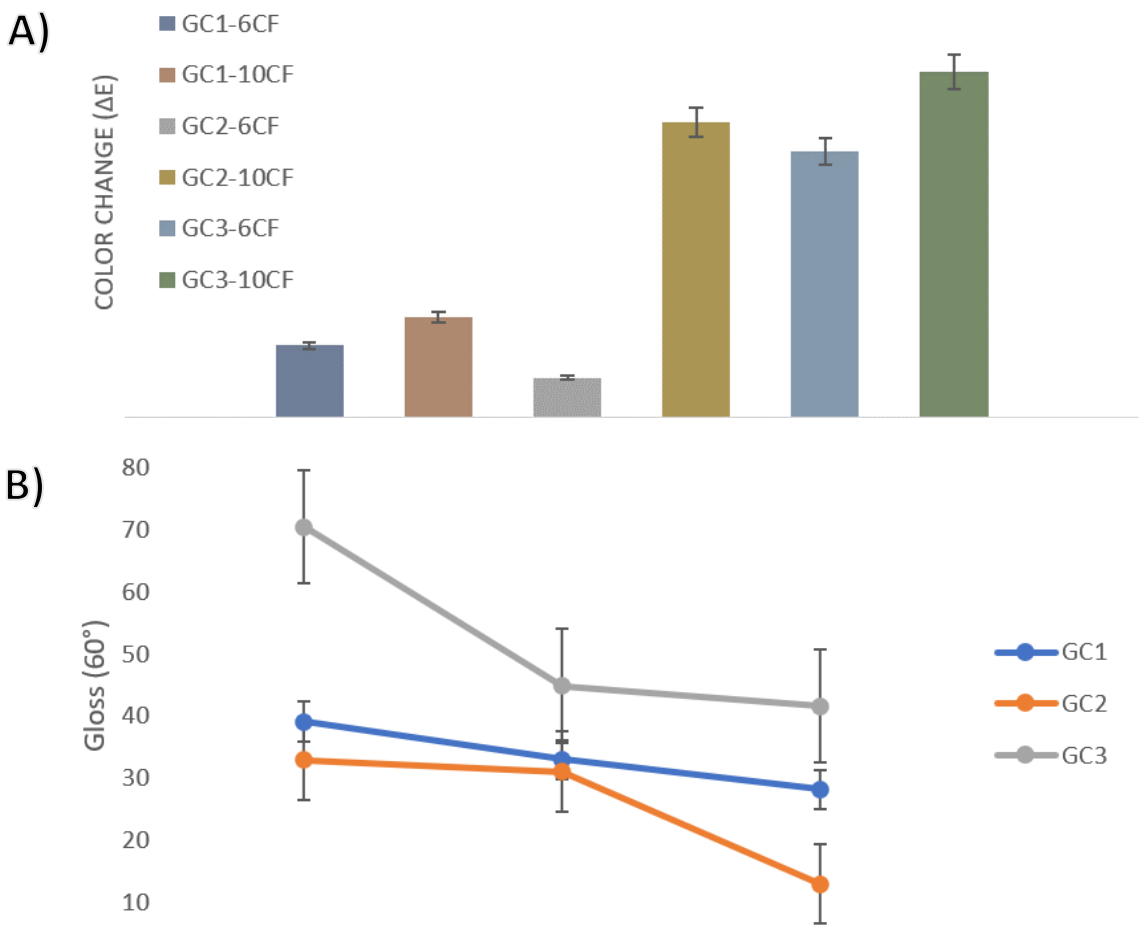

Figure 7. Gloss and color parameters of the studied samples. A) color changes of the studied samples B) gloss changes of the studied samples.

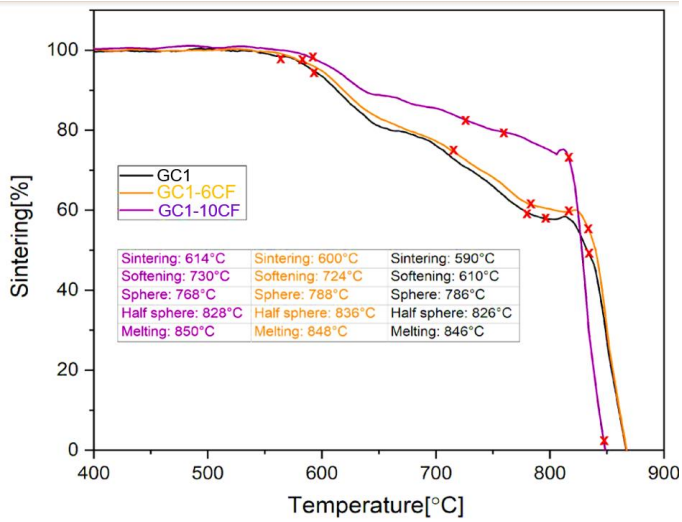

A)

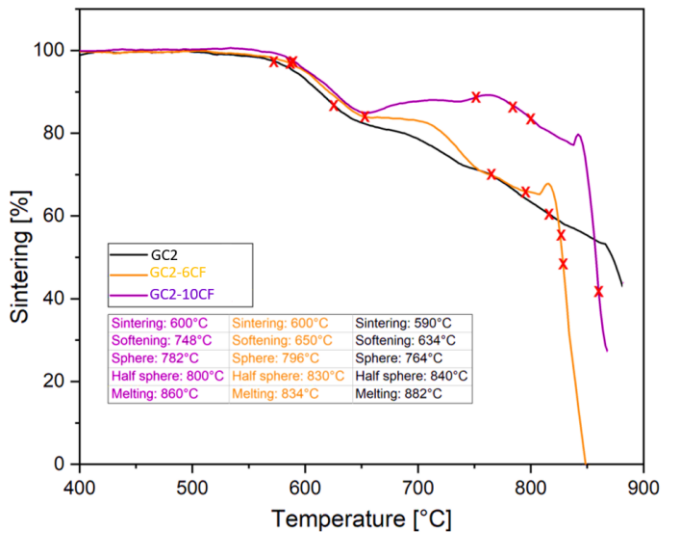

B)

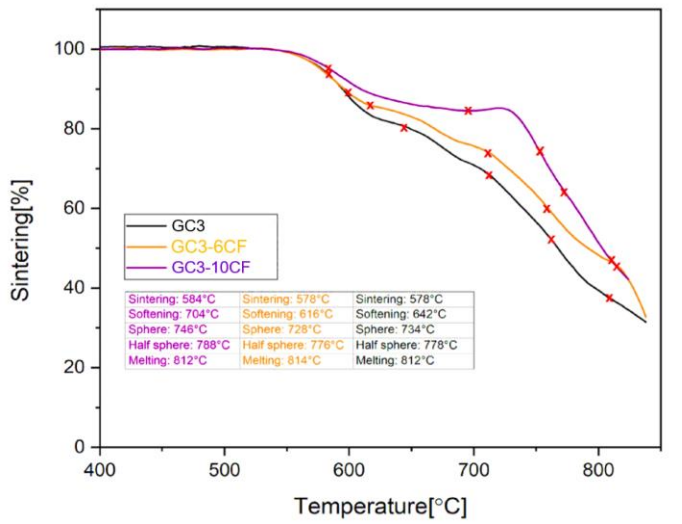

C)

Figure 8 Heating microscope analysis of the studied samples with different carbon fiber ratios. A) GC1 samples B) GC2 samples C) GC3 samples.

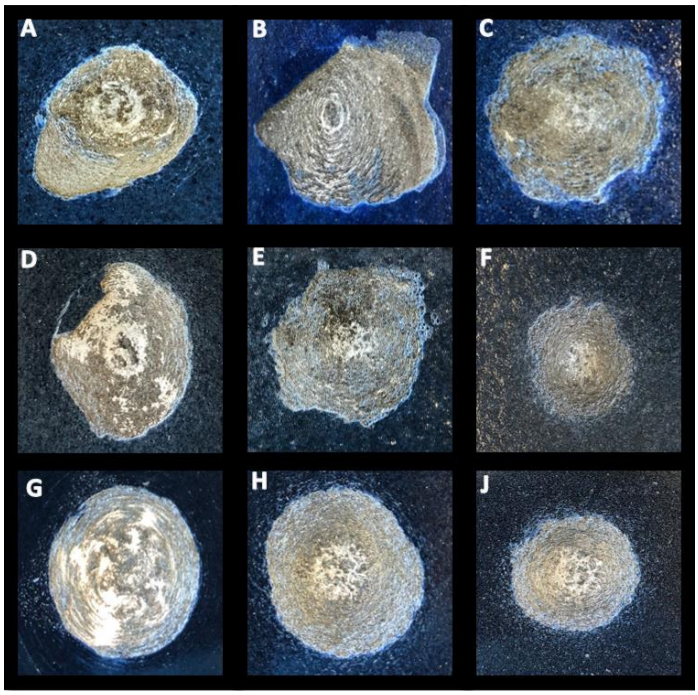

Figure 9. Results in impact test in A) GC1 B) GC1-6CF C) GC1-10CF D) GC2 E) GC2-6CF F) GC2-10CF G) GC3 H) GC3-6CF J) GC3-10CF.

4. CONCLUSIONS

In conclusion, the impact of carbon fiber used on the structural properties of glass-ceramic coatings was addressed in this work. Two different numbers of fibers were considered. When the carbon fiber ratio is 1% wt., the hardness of GC1 samples increases from 737.4 to 763.8 VH In GC2 samples, the hardness is increased from 816.6 to 889 VH when the carbon fiber ratio is 1% wt. In GC3 samples, the hardness is increased from 831.6 to 865.2 VH when the carbon fiber ratio is 1% wt. Carbon fiber is effective in increasing the disorder of the surface of glass-ceramic coatings, resulting in a loss of aesthetic characteristics for each formulation. The thermal and phase formation behavior of glass-ceramic coatings is unaffected by the fibers. However, carbon fiber changes the characteristic temperatures obtained by heating microscope analysis, also the addition of 1%CF to GC3 causes to enhance thermal properties of the sample. The quantity of carbon fiber investigated in this study does not affect the adherence properties of the samples. This study aimed to enhance the hardness values of the coatings; hence the best hardness increase was obtained in GC2. In addition, less color changes were obtained in GC2-6.

According to the findings:

- Carbon fiber in the glass-ceramic coating increases hardness, and as the fiber content increases, the hardness increases as well.
- Carbon fiber can be incorporated into glass-ceramic coatings.
- However, this incorporation needs further research, and future research should also concentrate on tailoring carbon fiber to prevent oxidation.

References

[1] M. H. Lewis, J. Metcalf-Johansen, P. S. Bell "Crystallization Mechanisms in Glass-Ceramics," *Management*, **62** (5-6) 278–288 (1979).

[2] Wolfram Holand, *Glass-Ceramic Technology* (2002).

[3] G. A. Khater, E. M. Safwat, J. Kang, Y. Yue, and A. G. A. Khater, "Some Types of Glass-Ceramic Materials and their Applications," *Int. J. Res. Stud. Sci. Eng. Technol.*, **7** (3) 2349–476 (2020).

[4] D. Wang, "Effect of crystallization on the property of hard enamel coating on steel substrate," *Appl. Surf. Sci.*, **255** (8) 4640–4645 (2009).

[5] I. W. Donald, P. M. Mallinson, B. L. Metcalfe, L. A. Gerrard, and J. A. Fernie, "Recent developments in the preparation, characterization, and applications of glass- and glass-ceramic-to-metal seals and coatings," *J. Mater. Sci.*, **46** (7) 1975–2000 (2011).

[6] M. Chen, W. Li, M. Shen, S. Zhu, and F. Wang, "Glass coatings on stainless steels for high-temperature oxidation protection: Mechanisms," *Corros. Sci.*, **82**, 316–327, 2014.

[7] V. A. Rozenenkova, S. S. Solntsev, D. V. Grashchenkov, and N. A. Mironova, "Glass-Ceramic Coatings for Protecting Steel From Interaction with Hydrogen," *Glas. Ceram. (English Transl. Steklo i Keramika)*, **72** (11–12) 430–434 (2016).

[8] E. Scrinzi and S. Rossi, "The aesthetic and functional properties of enamel coatings on steel," *Mater. Des.*, **31** (9) 4138–4146 (2010).

[9] S. Rossi, F. Russo, and M. Calovi, "Durability of vitreous enamel coatings and their resistance to abrasion, chemicals, and corrosion: a review," *J. Coatings Technol. Res.*, **18** (1) 39–52 (2021).

[10] W. Eitel, *Silicate Science*, 1976.

[11] S. Rossi, N. Parziani, and C. Zanella, "Abrasion resistance of vitreous enamel coatings in the function of frit composition and particles presence," *Wear*, **332–333**, 702–709 (2015).

[12] B. Xu, E. Wang, W. Gong, and X. Yue, "Preparation of glass-ceramics of Li2O-Al2O3-ZnO-SiO2 system coating toughed by ZrO2 basic on a metal substrate," *Adv. Mater. Res.*, **602–604**, 1630–1634 (2013).

[13] S. Rossi, N. Gasparre, V. Fontanari, and A. Compagnoni, "Modification of the mechanical properties of vitreous enameled aluminum substrate adding graphene flakes," *Key Eng. Mater.*, **813**, 49–54 (2019).

[14] S. Rossi, M. Fedel, F. Deflorian, and N. Parziani, "Abrasion and chemical resistance of composite vitreous enamel coatings with hard particles," *Surf. Interface Anal.*, **48** (8) 827–837 (2016).

[15] R. Syed, "Heat conduction characteristics of a carbon-fiber-reinforced lithia-alumino-silicate glass-ceramic," **22**, 701–709 (1987).

[16] W. Sinkler, M. Monthioux, V. Bianchi, P. Goursat, and E. Ménessier, "Carbon fiber-reinforced (YMAS) glass-ceramic matrix composites. II. Structural changes in the matrix with temperature," *J. Eur. Ceram. Soc.*, **19** (3) 305–316 (1999).

[17] S. Wu *et al.*, "Co-enhancement of oxidation resistance and mechanical properties of Cf/LAS composites: The effects of h-BN addition," *J. Eur. Ceram. Soc.*, **40** (1) 19–27 (2020).

[18] V. Bianchi, P. Goursat, W. Sinkler, M. Monthioux, and E. Ménessier, "Carbon-fibre-reinforced (YMAS) glass-ceramic matrix composites. I. Preparation, structure and fracture strength," *J. Eur. Ceram. Soc.*, **17** (12) 1485–1500, (1997).

[19] X. H. Zheng, Y. G. Du, J. Y. Xiao, W. J. Zhang, and C. Y. Liang, "Effect of sintering temperature on BaO-Al2O3-SiO 2 glass-ceramic coating for carbon fiber reinforced silicon carbide matrix composites," *Mater. Sci. Technol.*, **24** (11) 1399–1402 (2008).

[20] S. Wu *et al.*, "The evolution of carbon fibers with Fe 3+ doping and effects on the mechanical properties of C f /BAS composites," *Compos. Part B Eng.*, **163**, 447–454 (2019).

[21] V. Bianchi, P. Goursat, W. Sinkler, M. Monthioux, and E. Ménessier, "Carbon fiber-reinforced (YMAS) glass-ceramic matrix composites. III. Interfacial aspects," *J. Eur. Ceram. Soc.*, **19** (3) 317–327 (1999).

[22] V. Bianchi, P. Fournier, F. Platon, and P. Reynaud, "Carbon fiber-reinforced (YMAS) glass-ceramic matrix composites: Dry friction behavior," *J. Eur. Ceram. Soc.*, **19** (5) 581–589 (1999).

[23] V. Bianchi, P. Goursat, and E. Ménessier, "Carbon-fiber-reinforced ymas glass-ceramic-matrix composites - IV. Thermal residual stresses and fiber/matrix interfaces," *Compos. Sci. Technol.*, **58** (3–4) 409–418 (1998).

[24] S. Reinsch, C. Reich, and R. Brückner, "Optimized preparation parameters of unidirectionally C fibre-reinforced glass ceramics of the systems MAS and BMAS," *J. Mater. Sci.*, **30** (22) 5632–5638 (1995).

[25] F. Ye, L. Liu, and L. Huang, "Fabrication and mechanical properties of carbon short fiber reinforced barium aluminosilicate glass-ceramic matrix composites," *Compos. Sci. Technol.*, **68** (7–8) 1710–1717 (2008).

[26] L. Xia, X. Wang, G. Wen, X. Li, C. Qin, and L. Song, "Influence of brick pattern interface structure on mechanical properties of continuous carbon fiber reinforced lithium aluminosilicate glass-ceramics matrix composites," *J. Eur. Ceram. Soc.*, **32** (2) 409–418 (2012).

[27] D. Boccaccini, M. Cannio, E. Bernardo, A.R. Boccaccini, "Glass and Glass-Ceramic Matrix Composites for Advanced Applications: Part I: Properties and Manufacturing Technologies," *Encyclopedia of Materials: Technical Ceramics and Glasses*, **2**, 277-287 (2021).

[28] E. Bernardo, "Glass Matrix Composite," *Wiley Encycl. Compos.*, (2011).

[29] F. Russo, S. Rossi, and A.M. Compagnoni. "Porcelain Enamel Coatings" *Encyclopedia*, **1** (2) 388-400 (2021).

[30] W. K. Tredway, K. M. Prewo, and C. G. Pantano, "Fiber-matrix interfacial effects in carbon-fiber-reinforced glass matrix composites," *Carbon*, **27** (5) 717–727 (1989).

[31] H. H. Momsen, "A Guide to Understanding Color," *Printwear*, **18** (8) 32–36 (2005).

[32] L. Samiee, H. Sarpoolaky, and A. Mirhabibi, "Influence of bubble structure on adherence and chemical durability of porcelain enamel," *Adv. Appl. Ceram.*, **107** (1) 27–33 (2008).

[33] K. Maeda, K. Akatsuka, G. Okuma, and A. Yasumori, "Mechanical properties of CaO-Al2O3-SiO2 glass-ceramics precipitating hexagonal $CaAl_2Si_2O_8$ crystals," *Crystals*, **11** (4) 1–12 (2021).

[34] I. Hervas, A. Montagne, A. Van Gorp, M. Bentoumi, A. Thuault, and A. Iost, "Fracture toughness of glasses and hydroxyapatite: A comparative study of 7 methods by using Vickers indenter," *Ceram. Int.*, **42** (11) 12740–12750 (2016).

[35] W. Han, "Glass ceramic of high hardness and fracture toughness developed from iron-rich wastes," *Acta Metall. Sin. (English Lett.)*, **22** (3) 181–190 (2009).

[36] I. Žmak, D. Ćorić, V. Mandić, and L. Ćurković, "Hardness and indentation fracture toughness of slip cast alumina and alumina-zirconia ceramics," *Materials*, **13** (1) 122, 1–17 (2020).

[37] I. S. Gutzow and J. W. P. Schmelzer, *Kinetics of Overall Crystallization: Kinetic Criteria for Glass-Formation BT - The Vitreous State: Thermodynamics, Structure, Rheology, and Crystallization*, Springer, Second Edit. 2013.